

Theory of dense hydrogen

S. Chakravarty, J. H. Rose, D. Wood, and N. W. Ashcroft

Laboratory of Atomic and Solid State Physics, Cornell University, Ithaca, New York 14853

(Received 5 January 1981)

Equations of state for molecular and metallic hydrogen are calculated in an accurate and comparable manner by using the density-functional method applied to static lattices. By isolating the electronic energies in this way, attention can be drawn to the relative importance of the protonic degrees of freedom. From the equation-of-state results it can be concluded that a remnant molecular pairing is preferred in a band-overlap metallic state, complete dissociation occurring only at very high densities ($r_s \sim 1.1$). An accurate determination of the pressure needed to achieve complete dissociation is shown to require a self-consistent treatment of electron and proton degrees of freedom.

I. INTRODUCTION

In understanding the transition of hydrogen to a metal at high pressures we face a problem of considerable theoretical difficulty. Even the qualitative mechanism for the transition has not been fully determined. There are two likely candidates for a solid-solid transition.¹ First, as the hydrogen is compressed it catastrophically loses its diatomic (molecular) character at some point and forms a solid with an odd number of electrons per unit cell.² The simplest result would be a metallic solid with one electron per basis site. However, there is a second mechanism for the transition which may occur at lower pressure: This is a band-overlap metalization, in which the solid remains diatomically ordered.^{3,4}

The purpose of this paper is to consider the energetics of both possibilities. We provide a detailed comparison of the ground-state energies of the monatomic and diatomic phases primarily within the static lattice approximation. Estimates are obtained for the diatomic to monatomic transition pressure, the equations of state for diatomic (molecular) and monatomic hydrogen at high pressures, and the interproton spacing and approximate optic-mode energy of the "molecular" or diatomically ordered phase. We test the sensitivity of our results to the static lattice approximation by introducing phonons in a reasonable but nevertheless approximate way. At high pressures our results are generally insensitive to their inclusion, with the important exception that the transition pressure for complete dissociation of the diatomic phase depends crucially on the detailed model for the phonons. At low pres-

ures we verify that inclusion of the phonon degrees of freedom is essential for a proper understanding of the equation of state of the molecular solid. An important conclusion is that the determination of the equation of state at low pressures and the diatomic-to-monatomic transition pressure at high pressures require a calculation in which *both* the electron and ion degrees of freedom are included self-consistently.

Currently, most calculations of the thermodynamic properties of hydrogen at high pressures treat the monatomic and diatomic phases in quite different ways. For example, the properties of the metallic monatomic phase are often obtained by low-order perturbation theory about the uniform electron gas. On the other hand, the diatomic phase is often treated in the pair potential approximation. As emphasized by Ross and McMahan⁵ such disparate techniques make comparison between the consequent equations of state an inherently imprecise procedure since the inevitable errors also enter in quite different ways.

The density-functional theory of Kohn and Sham⁶ provides the basis for a unified treatment of both phases. It is now known that with care an application of this technique can provide excellent results for inhomogeneous or localized systems such as atoms and molecules, and for electronically delocalized systems such as metals and metal surfaces.⁷ For a periodic system the essence of the technique is to minimize the energy functional with respect to a set of single-particle wave functions which satisfy the standard periodic boundary conditions. Thus a straightforward but very laborious way to proceed for crystalline systems is to carry out a self-

consistent band-structure calculation [as a function of $r_s = (\frac{4}{3}\pi\bar{\rho}a_0^3)^{-1/3}$, where $\bar{\rho}$ is the mean electron density and a_0 is the Bohr radius] for all the plausible crystallographic structures in each phase.

A more practical approach, however, is to proceed by performing self-consistent band-structure calculations within a *spherical* Wigner-Seitz (WS) cell. Evidently this is quite reasonable for the monatomic phase where the differences in crystallographic structure account for exceedingly small energy differences, of the order of 1 mRy per proton. By itself a spherical calculation of each molecule in the *diatomic* phase would not appear to make much sense (in fact, however, we shall see that for an isolated H_2 molecule this procedure nevertheless gives $\sim 90\%$ of the ground-state energy). The hydrogen molecules, though spherical in their rotational ground states, are certainly not spherical on the important time scale of electronic rearrangements.⁸ We therefore proceed here in the following way: First we solve the diatomic system by using a spherical Wigner-Seitz cell which encloses each molecule. The potential of the molecule is initially averaged over rotations. Then we use perturbation theory to restore the molecule to its original intracellular symmetry. This perturbation theory requires at least the linear and first *nonlinear* response functions of the *nonuniform* but spherical molecular system calculated above. Taking the system thus defined to the low-density limit ($r_s \rightarrow \infty$) we obtain the isolated H_2 molecule. Here our estimates for the vibrational frequency, the interproton spacing, and the dissociation energy agree closely with experiment and also with detailed theoretical calculations by different methods. This indicates that the perturbation scheme converges well and can be expected to be physically meaningful at higher densities, where the electron density is more nearly uniform.

The structure of the paper is as follows. Section II details the density-functional calculation of the ground-state energy of the monatomic phase within the static lattice approximation. The third section describes our calculational procedure for the diatomically ordered phase. The fourth and fifth sections give the static lattice results for monatomic and diatomic hydrogen, respectively. Section VI deals with estimates of the phonon corrections to the static results and establishes the importance of phonon energies on the scale of electronic *binding* energies in the static lattice calculations. The final section is devoted to a discussion of the major results and includes a brief comparison with the

structural expansion approach applied to the same model.

That band overlap metallization of dense hydrogen is a distinct possibility is borne out by our results. Friedli and Ashcroft⁴ have obtained an estimate of the band overlap transition density as a function of the molecular interproton spacing, $2d$. Using the results we shall describe below for the calculated value of the interproton spacing, we find an estimate of ~ 2 Mbar for a metal-insulator transition arising from band overlap. The insulator-metal transition therefore appears to be manifested first in a diatomically ordered state of the crystal, and, as we shall see, only at much higher pressures is the diatomic order completely lost.

II. THE CONDENSED MONATOMIC STATE

The method we describe is similar to that used by Tong.⁹ We proceed by first centering a Wigner-Seitz (WS) sphere of radius $r_{ws}a_0$ on each site of a close-packed solid. As noted above this assumes that to a good approximation the ground-state energy depends only on the atomic volume and not on the crystal structure.¹⁰ For an external potential $v_{ext}(\vec{r})$ the Kohn-Sham self-consistent scheme can be summarized in the following equations. The energy functional is

$$E[\rho] = T_s[\rho] + E_{xc}[\rho] + \int \rho(\vec{r})v_{ext}(\vec{r})d\vec{r} + \frac{1}{2}e^2 \int d\vec{r} \int d\vec{r}' \frac{\rho(\vec{r})\rho(\vec{r}')}{|\vec{r} - \vec{r}'|}, \quad (2.1)$$

where E is now the total energy of all the electrons in a single cell which contains a stationary proton at its center. In (2.1) $E_{xc}[\rho]$ is the exchange-correlation energy functional of the interacting electron gas. In the local approximation,¹¹ it is given by

$$E_{xc}[\rho] = \int \epsilon_{xc}(\rho(\vec{r}))\rho(\vec{r})d\vec{r}, \quad (2.2)$$

where $\epsilon_{xc}(\rho(\vec{r}))$ is the exchange and correlation energy per electron of a *uniform* electron gas of local density $\rho(\vec{r})$. All integrations in Eqs. (2.1) and (2.2) are limited to the WS cell. The quantity $T_s[\rho]$ is the single-particle kinetic-energy functional of electrons in an effective single-particle potential v_{eff} satisfying

$$\left[-\frac{\hbar^2}{2m}\nabla^2 + v_{eff}(\vec{r}) \right] \Psi_{\vec{k}}(\vec{r}) = \epsilon_{\vec{k}}\Psi_{\vec{k}}(\vec{r}), \quad (2.3)$$

$$r < r_{ws},$$

with the boundary conditions

$$\Psi_{\vec{k}}(\vec{r}) = \exp(i2ka_0r_{\text{WS}} \cos\theta)\Psi_{\vec{k}}(-\vec{r}) \Big|_{r=r_{\text{WS}}} \quad (2.4)$$

and

$$\frac{\partial\Psi_{\vec{k}}(\vec{r})}{\partial r} = -\exp(i2ka_0r_{\text{WS}} \cos\theta) \frac{\partial\Psi_{\vec{k}}(-\vec{r})}{\partial r} \Big|_{r=r_{\text{WS}}}, \quad (2.5)$$

where r_{WS} is the Wigner-Seitz radius and $\cos\theta = \hat{r} \cdot \vec{k}$. In Eq. (2.3)

$$v_{\text{eff}}(\vec{r}) = v_{\text{ext}}(\vec{r}) + e^2 \int \frac{\rho(\vec{r}')}{|\vec{r} - \vec{r}'|} d\vec{r}' + \mu_{\text{xc}}(\rho(\vec{r})), \quad (2.6)$$

where

$$\mu_{\text{xc}}(\rho(\vec{r})) = \frac{d}{d\rho} [\rho\epsilon_{\text{xc}}(\rho)]. \quad (2.7)$$

The self-consistent solution of Eqs. (2.3)–(2.6) now gives the ground-state energy from Eq. (2.1). The exchange-correlation energy functional of Gunnarsson and Lundqvist¹² has been used in the present calculation. In the case of hydrogen, a paramagnetic energy functional then leads to a half filled band, i.e., a metallic state. The calculation has also been repeated, however, with a spin-aligned or “ferromagnetic” energy functional whose form can also be found in Ref. 12. This leads to an insulating phase which is found to be energetically preferred (to the paramagnetic phase) at low densities. The case of a simple isolated hydrogen atom can be obtained by taking the limit $r_{\text{WS}} \rightarrow \infty$. This will be discussed below.

III. THE CONDENSED DIATOMIC STATE

The calculation for the molecular solid is not as straightforward as the procedure just described. The system cannot be reduced to the single-cell problem in a particularly simple way. In order to take advantage of the density-functional theory we carry out the following steps. First, we isolate the part of the Hamiltonian which contributes most to the ground-state energy. Instead of considering two point charges (protons) separated by a distance $2d$ and located about a lattice point, we construct a

more symmetric problem by smearing the charges on a spherical shell of radius d . Put another way, we consider the *spherical* average of the interaction between an electron and two protons.¹³ The corresponding unscreened interaction seen by an electron is shown in Fig. 1. Note that d is to be considered as a variational parameter in what follows and is not restricted to its normal molecular value of 0.37 Å. This spherically averaged interaction may be written as

$$v_{\text{sph}} = -\frac{2e^2}{(r,d)_>}. \quad (3.1)$$

[We introduce the notation $(x,y)_>$ as the larger of the two variables x and y . Similarly $(x,y)_<$ will mean the smaller of the two variables.]

Imagine now replacing the two protons located about each lattice site by a spherical shell of charge in the manner described above. From the periodicity of the lattice, the problem can again be reduced to a charge-neutral single-cell problem containing on the average two electrons and having no multipole moments outside the cell. This procedure again ignores structural energies of the order of millirydbergs and is justified by comments similar to those usually advanced for the monatomic case. The Kohn-Sham density-functional calculation can now be repeated with v_{ext} replaced by v_{sph} in Eq. (3.1), and with the exchange correlation energy functional taken to be the paramagnetic form. As we shall see in detail below, this accounts for about the 90% of the total ground-state energy at $r_s \sim 2.0$. We are now in a position to develop a perturbation theory in orders of $\Delta v = v_{\text{ext}} - v_{\text{sph}}$. If we call $E_0(r_s)$ the energy corresponding to the spherically averaged

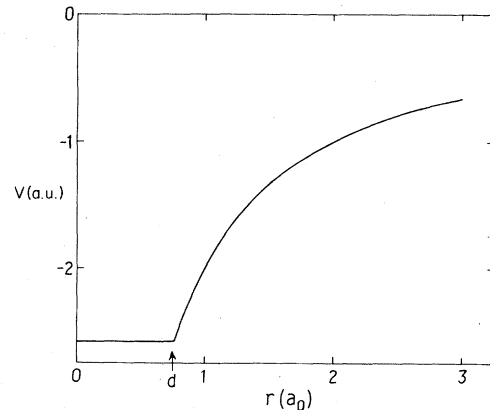


FIG. 1. Spherically averaged unscreened potential for electrons in the presence of a pair of protons separated by $2d$.

potential v_{sph} , then the total ground-state energy can be written as

$$E(d, r_s) = E_0(d, r_s) + \Delta E^{(1)}(d, r_s) + \Delta E^{(2)}(d, r_s) + \Delta E^{(3)}(d, r_s) + \dots, \quad (3.2)$$

where

$$\Delta E^{(1)}(d, r_s) = \int \Delta v(\vec{r}) \rho^0(\vec{r}) d\vec{r}, \quad (3.3)$$

$$\Delta E^{(2)}(d, r_s) = \frac{1}{2} \int d\vec{r}_1 \int d\vec{r}_2 \Delta v(\vec{r}_1) \Delta v(\vec{r}_2) \times \chi^{(1)}(\vec{r}_1, \vec{r}_2), \quad (3.4)$$

$$\Delta E^{(3)}(d, r_s) = \frac{1}{3} \int d\vec{r}_1 \int d\vec{r}_2 \int d\vec{r}_3 \Delta v(\vec{r}_1) \Delta v(\vec{r}_2) \Delta v(\vec{r}_3) \times \chi^{(2)}(\vec{r}_1, \vec{r}_2, \vec{r}_3). \quad (3.5)$$

In these equations $\rho^0(\vec{r})$ in Eq. (3.3) denotes the spherical density calculated in the zeroth order (i.e., with v_{sph}). The quantities $\chi^{(1)}$ and $\chi^{(2)}$ are the appropriate response functions to be described in detail below. It is immediately clear that $\Delta E^{(1)} = 0$. The fact that the unperturbed (or zero-order) Hamiltonian was chosen in such a way that the first-order perturbation correction vanishes is one of the main reasons why E_0 accounts for most of the total energy and in particular most of the electrostatic energy. We next describe in detail the physical content of Eqs. (3.2)–(3.5). First the perturbing potential $\Delta v(\vec{r})$ is given by

$$\begin{aligned} \Delta v(\vec{r}) &= -\frac{e^2}{|\vec{r} - \vec{d}|} - \frac{e^2}{|\vec{r} + \vec{d}|} + \frac{2e^2}{(r, d)_>} \\ &= -2e^2 \sum_{l=2,4,6,\dots} \frac{(r, d)_{<}^l}{(r, d)_{>}^{l+1}} P_l(\hat{r} \cdot \hat{d}), \end{aligned} \quad (3.6)$$

where, as noted above, we have two protons situated at a distance d from the center of the cell. In the system under consideration the electron gas is inhomogeneous and little is known about the screened density-density response function $\chi^{(1)}$. Accordingly we invoke a simple but reasonable *nonlocal* ansatz to be used in the spirit of the local-density approximation. Let $\chi_H^{(1)}$ be the commonly used linear response function of a homogeneous system of electrons responding to an *external* potential. We then approximate $\chi^{(1)}$ by

$$\chi^{(1)}(\vec{r}_1, \vec{r}_2) \approx \chi_H^{(1)} \left(r_{12}; \frac{\rho(\vec{r}_1) + \rho(\vec{r}_2)}{2} \right), \quad (3.7)$$

i.e., the exact $\chi^{(1)}(\vec{r}_1, \vec{r}_2)$ is replaced by the corresponding function for the homogeneous system but with a density intermediate between those corresponding to positions r_1 and r_2 ($r_{12} = |\vec{r}_1 - \vec{r}_2|$). This should be quite accurate for most of the regions of the configuration space and we justify it *a posteriori* by examining the results for molecular hydrogen in the low-density limit. An expansion in Legendre polynomials then gives

$$\Delta E^{(2)}(d, r_s) = 16e^4 \sum_{l=2,4,6,\dots} \frac{1}{2l+1} \int_0^{r_{\text{ws}}} dr_1 r_1^2 \frac{(r_1, d)_{<}^l}{(r_1, d)_{>}^{l+1}} \int_0^{r_{\text{ws}}} dr_2 r_2^2 \frac{(r_2, d)_{<}^l}{(r_2, d)_{>}^{l+1}} K_l(r_1, r_2), \quad (3.8)$$

where

$$r_s = 2^{-(1/3)} r_{\text{ws}},$$

and

$$K_l(r_1, r_2) = \int_0^\infty dq q^2 j_l(qr_1) j_l(qr_2) \chi_H^{(1)} \left(q; \frac{\rho(\vec{r}_1) + \rho(\vec{r}_2)}{2} \right). \quad (3.9)$$

Because of the presence of the oscillating spherical Bessel functions $j_l(qr)$, the convergence of Eq. (3.8) is very rapid and in fact the omission of $l \geq 10$ causes negligible error. The response function $\chi_H^{(1)}$ is taken as

$$\chi_H^{(1)}(q, \rho) = \frac{\chi_0(q, \rho)}{1 - \chi_0(q, \rho) \left[\frac{4\pi e^2}{q^2} + \frac{d^2}{d\rho^2} (\rho \epsilon_{\text{xc}}) \right]}, \quad (3.10)$$

which is the result for a uniform electron gas within Kohn-Sham theory. In Eq. (3.10) $\chi_0(q, \rho)$ is the Lindhard function corresponding to density ρ .

The third-order term is more complicated to evaluate and some essential simplification is necessary as will be explained below. In (3.5) we take a nonlocal approximation for $\chi^{(2)}(\vec{r}_1, \vec{r}_2, \vec{r}_3)$ given by

$$\chi^{(2)}(\vec{r}_1, \vec{r}_2, \vec{r}_3) \sim \chi_H^{(2)}\left(\vec{r}_{12}, \vec{r}_{13}, \vec{r}_{23}; \frac{\rho(\vec{r}_1) + \rho(\vec{r}_2) + \rho(\vec{r}_3)}{3}\right), \quad (3.11)$$

where the right-hand side of Eq. (3.11) is the response function of the homogeneous electron gas of density

$$\rho = \frac{1}{3}[\rho(\vec{r}_1) + \rho(\vec{r}_2) + \rho(\vec{r}_3)]. \quad (3.12)$$

We now replace $\chi_H^{(2)}$ by the corresponding quantity for the noninteracting electron gas, i.e.,

$$\begin{aligned} \chi_H^{(2)}(r_{12}, r_{13}, r_{23}) &= \frac{1}{(2\pi)^6} \int d\vec{k}_1 \int d\vec{k}_2 e^{i\vec{k}_1 \cdot \vec{r}_1 + i\vec{k}_2 \cdot \vec{r}_2 - i(\vec{k}_1 + \vec{k}_2) \cdot \vec{r}_3} \\ &\quad \times \chi_H^{(2)}(\vec{k}_1, \vec{k}_2, -\vec{k}_1 - \vec{k}_2), \end{aligned} \quad (3.13)$$

where

$$\begin{aligned} \chi_H^{(2)}(\vec{k}_1, \vec{k}_2 - \vec{k}_1, -\vec{k}_2) &= 2 \int \frac{d\vec{p}}{(2\pi)^3} n_p \left[\frac{1}{(\epsilon_{\vec{p}} - \epsilon_{\vec{p} + \vec{k}_1})} \frac{1}{(\epsilon_{\vec{p}} - \epsilon_{\vec{p} + \vec{k}_2})} \right. \\ &\quad \left. + \frac{1}{(\epsilon_{\vec{p}} - \epsilon_{\vec{p} + \vec{k}_1})(\epsilon_{\vec{p}} - \epsilon_{\vec{p} - \vec{k}_1 - \vec{k}_2})} + \frac{1}{(\epsilon_{\vec{p}} - \epsilon_{\vec{p} + \vec{k}_2})(\epsilon_{\vec{p}} - \epsilon_{\vec{p} - \vec{k}_1 - \vec{k}_2})} \right]. \end{aligned} \quad (3.14)$$

An asymptotic expansion in k space then provides an approximate $\chi_H^{(2)}(r_{12}, r_{13}, r_{23})$. The neglect of the small- k region contributes an error of the order of 5% in $\Delta E^{(3)}$ which in turn is only about 0.1% of the total energy. The justification for this approximation is that the large- k region dominates the behavior at short distances, and these are the most relevant regions for the integrand. The previous zero-order calculation obviously ignores the cusps in the electron density at the proton, and these cusps have their major contribution at large wave vector.

The resulting expansion for $\chi_H^{(2)}$ can be carried out very easily and yields

$$\chi_H^{(2)}(r_{12}, r_{23}, r_{31}) = \frac{m^2 k_F^3}{4\pi^4 n^2} \left[\frac{1}{|\vec{r}_1 - \vec{r}_3|} \frac{1}{|\vec{r}_2 - \vec{r}_3|} + \frac{1}{|\vec{r}_1 - \vec{r}_2|} \frac{1}{|\vec{r}_3 - \vec{r}_2|} + \frac{1}{|\vec{r}_3 - \vec{r}_1|} \frac{1}{|\vec{r}_1 - \vec{r}_2|} \right]. \quad (3.15)$$

The expression for $\Delta E^{(3)}$ can then be written as

$$\begin{aligned} \Delta E^{(3)} &= -96 \sum_{l,m,n=2,4,6,\dots} \frac{Q(l,m,n)}{(2l+1)(2m+1)} \\ &\quad \times \int_0^{r_{ws}} dr_1 r_1^2 \frac{(r_1, d)_{<}^l}{(r_1, d)_{>}^{l+1}} \\ &\quad \times \int_0^{r_{ws}} dr_2 r_2^2 \frac{(r_2, d)_{<}^m}{(r_2, d)_{>}^{m+1}} \int_0^{r_{ws}} dr_3 r_3^2 \frac{(r_3, d)_{<}^n}{(r_3, d)_{>}^{n+1}} \\ &\quad \times \left[\frac{(r_1, r_3)_{>}^l}{(r_2, r_3)_{>}^{l+1}} \frac{(r_2, r_s)_{<}^m}{r_2, r_3)_{>}^{m+1}} \right] \left[\frac{1}{r_s^3} \right], \end{aligned} \quad (3.16)$$

where

$$\frac{1}{r_s^3} = \frac{4}{9} \pi [n(r_1) + n(r_2) + n(r_3)].$$

Two of the threefold integrations can now be carried out analytically; the remaining one has to be disposed of numerically. The series is very rapidly convergent and its first 50 terms can actually be summed with little computing effort. The $Q(l, m, n)$ in (3.16) are given by the following expressions:

$$(a) \quad Q(l, m, n) = \int_{-1}^{+1} P_l(x)P_m(x)P_n(x)dx = 0 \quad \begin{array}{l} \text{unless } l + m + n = \text{even} \\ \text{and } l + m \geq n, \quad m + n \geq l, \quad n + l \geq m, \end{array} \quad (3.17)$$

$$(b) \quad Q(l, m, n) = \frac{2}{l + m + n + 1} \times \frac{\Gamma(l + m - n + 1)\Gamma(l + n - m + 1)\Gamma(m + n - l + 1)\Gamma^2\left(\frac{l + m + n}{2} + 1\right)}{\Gamma^2\left(\frac{l + m + n}{2} + 1\right)\Gamma^2\left(\frac{l + n - m}{2} + 1\right)\Gamma^2\left(\frac{m + n - l}{2} + 1\right)\Gamma(l + m + n + 1)}$$

otherwise .

The energy $E(d, r_s)$ can now be obtained by minimizing $E(d, r_s)$ with respect to d at a fixed value or r_s . The minimum gives the interproton energy as a function of density, and the curvature around this minimum then gives, in addition, a first estimate for the longitudinal optic-mode energy. This minimization is carried out because of a belief (which we shall see is substantially justified) that the interproton separation in the molecular solid at very high pressures can be quite different from that of the free molecule.

IV. MONATOMIC PHASE: STATIC LATTICE PROPERTIES

The total ground-state energy of monatomic H calculated within the static lattice approximation is shown by the solid line in Fig. 2. We discuss the results starting from the high-density regime. For sufficiently high density (small r_s) the system is a paramagnetic metal with a large positive energy, a consequence of the contribution from the kinetic energy. At $r_s = 1.65$ we find a minimum in the total energy whose value is $-1.09(6)$ Ry/proton thus yielding an approximate cohesive energy of $0.09(6)$ Ry/proton. There are two major sources of uncertainty in this estimate. First, estimates for the correlation energy differ by up to 20% for the range of densities of interest here. As an example, if we use the well-known expression of Nozieres and Pines,¹⁴ the cohesive energy is reduced to approximately 0.07 Ry/proton. Second, there are uncertainties in the value that should be attached to the energy in the limiting case of isolated hydrogen atoms. We have used the exact value of -1 Ry since this emerges from a self-interaction-corrected spin-density-functional calculation.

It is interesting to compare our results with those of the structural expansion method. Hammerberg and Ashcroft¹⁰ calculated the total energy to fourth order in the electron-proton interaction, and the correlation energy of the electron gas was given by the Nozieres-Pines interpolation formula. Exchange and correlation effects were not included, however, in the various response functions appearing in their theory. The minimum ground-state energy was

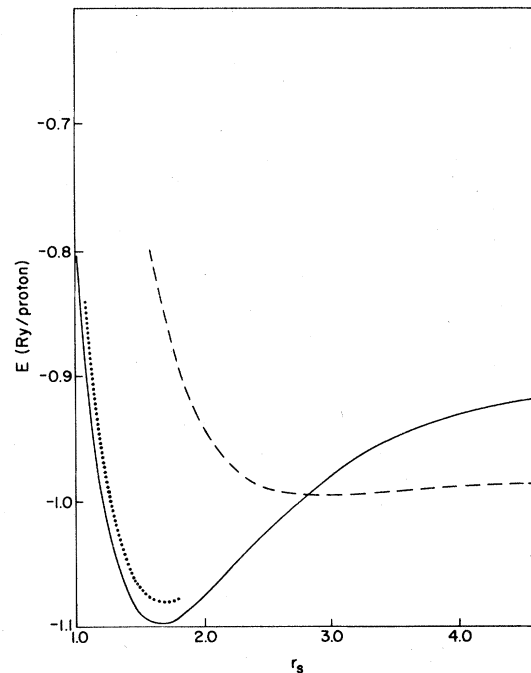


FIG. 2. Total ground-state energy of a static lattice, paramagnetic monatomic phase of metallic hydrogen as a function of r_s (solid line). The dashed curve represents the corresponding energy for a spin-polarized system. The dotted line is the solid curve augmented by phonon zero-point energy (see text).

found to be -1.044 Ry/proton. But note now that if we use Eq. (3.10) to introduce exchange and correlation into the response function of the second-order term, and assume that the third- and fourth-order terms are similarly affected, we obtain a minimum energy of -1.054 Ry/proton. When our own static lattice results are changed to reflect the Nozieres-Pines correlation energy, and the bcc Madelung energy is used (instead of the ion-sphere result), we find a value of $-1.06(9)$ Ry/proton.

Though the absolute energies obtained by these very different methods are thus in quite close agreement, there remain variations of up to 30% in the predicted cohesive energies, the uncertainties residing mostly in the choice of the correlation energy functional. Though systematic errors (between diatomic and monatomic phase calculations) can be reduced, it seems unlikely that absolute errors at the 1% level can be further reduced using self-consistent field theories. Higher accuracy may well be possible, however, through the use of fully correlated many-body wave functions in a Jastrow-function method.

The system undergoes a transition from paramagnetic to ferromagnetic order at $r_s \approx 2.8$. Within a self-consistent band-structure approach, the paramagnetic phase has two half-filled spin bands and is a metallic state. On the other hand, the ferromagnetic phase has a single spin filled band. The other spin band lies above the normal Fermi energy, and hence the ferromagnetic phase represents an insulating state. We thus find a metal-insulator transition when the protons are constrained to lie on a monatomic lattice (see Fig. 2). This point has been emphasized previously.¹⁵ In a more complete calculation Rose *et al.*¹⁶ found that there are two transitions near $r_s = 2.8$. The first is at $r_s = 2.74$, where there is a second-order transition involving the change of the paramagnetic metal to a spin-ordered metal. The second reported transition is a first order metal-insulator transition at $r_s = 2.84$. There the transition is from a spin-ordered metal to a ferromagnetic insulator.

The low-density limit of monatomic hydrogen is the isolated H atom. For large values of r_s we find the energy reaches an asymptotic value of -0.982 Ry. This is just the value which one finds for H within spin-density functional theory.¹⁷ The deviation of this value from -1 Ry typifies the limitations of density-functional theory in calculating total energies. However, relative energy differences are generally calculated much more accurately. This will become evident when we discuss the cal-

culational for the H_2 molecule, which is the low-density limit of our model of the diatomic phase.

Aside from the total energy, the pressure-density curve is the most interesting result for the monatomic phase. For $r_s > 1.65$ the pressure is negative, indicating that the solid wishes to relax to the energy minimum. The results for $r_s < 1.65$ are shown by the solid line in Fig. 3.

V. DIATOMIC PHASE: STATIC LATTICE RESULTS

A. Total energy and equation of state

The static lattice results for the ground-state energy (3.2) of the molecular phase are shown as the full curve in Fig. 4. The salient features are as follows: (i) there is a sharp rise in energy at high densities (or small r_s), (ii) there is a minimum at $r_s = 2.1$ with a value $E_{\min} = -1.173$ Ry/proton, and (iii) there is an asymptotic value for the energy in the limit that r_s becomes large. This limit is $E = -1.158$ Ry/proton. We analyze the low-density results first for two reasons: First, to establish the convergence of our perturbation expansion for the static lattice cases, and second, to show by comparison with experiment that the static lattice approximation *cannot* describe the equation of state for low-pressure hydrogen in a reasonable way.

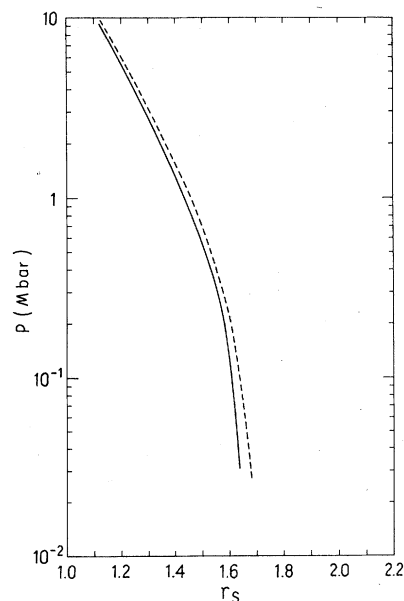


FIG. 3. Equation of state ($T = 0$) for monatomic paramagnetic metallic hydrogen (full line). The dashed curve includes contributions from proton dynamics.

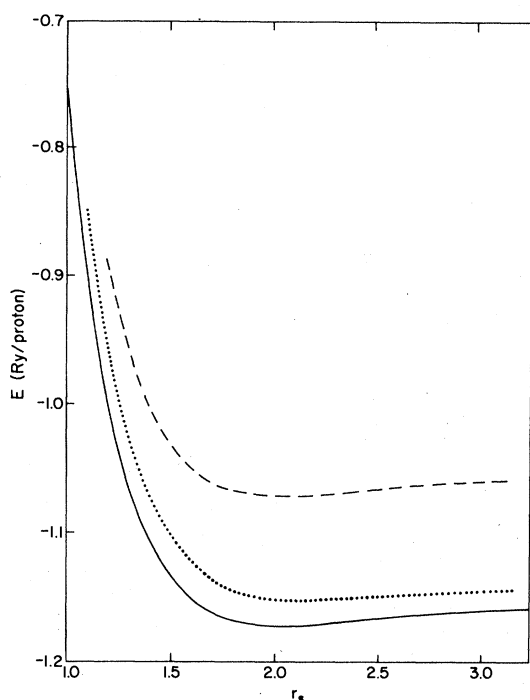


FIG. 4. Total ground-state energy of diatomically ordered solid molecular hydrogen: dashed line E_0 , full line $E_0 + \Delta E^{(2)} + \Delta E^{(3)}$. The dotted curve is the full curve augmented by phonon zero-point energies (see text).

The low-density limit of our calculation corresponds physically to a collection of isolated H_2 molecules. The calculation in this limit is a rather severe check on the convergence of our perturbation expansion, since we start with bare electrons and protons and do not parametrize the molecular data in any way. By comparing our calculated energy for the molecule with that of the hydrogen atom computed in the Kohn-Sham scheme, we find a dissociation energy of 0.348 Ry. This falls within 0.3% of the dissociation energy as determined both by experiment and also by quite detailed variational calculations.¹⁸ Results to the same accuracy are found for the optic mode vibrational frequency and the interproton spacing (see Table I). In some

TABLE I. Relative semiproton-spacing, d , and optic mode energy as a function of density, r_s .

$r_s (T = 0)$	$(d/a_0 r_{WS})$	$\frac{1}{2} \hbar \omega_{opt}$ (Ry/proton)
1.00	0.417	0.018
1.10	0.404	0.0167
1.20	0.391	0.0150
1.30	0.377	0.0137
1.50	0.349	0.0119
1.65	0.329	0.0110
1.85	0.301	0.0104
2.00	0.282	0.0099
2.15	0.264	0.0099
2.35	0.242	0.0098
2.50	0.227	0.0097
2.75	0.205	0.0099
3.10	0.182	0.0099

respects, the molecular limit is the extreme of inhomogeneity in the present calculation. The convergence of the perturbation expansion should become increasingly better at higher densities since the electronic density becomes correspondingly more uniform. Table II shows the results to third order for a sequence of different densities.

An additional comment may be made regarding the accuracy of these static lattice results. Our calculation is based on a spherical WS cell. For the monatomic phase it has been shown that this approximation leads to structural corrections on the order of 1 mRy which are negligible for our purposes. These corrections are also negligible for the diatomic phase as we can see as follows.

Consider a multipole expansion of the electrostatic potential associated with a single cell, which we take to have cubic symmetry. The cell is neutral and the crystal on average has inversion symmetry. As a consequence the dipole contribution to the potential vanishes. In addition we have cubic symmetry and so the quadrupole contribution will also vanish. (For a noncubic crystal the term will also

TABLE II. Energies in the diatomic phase, to third order (the energies quoted here are obtained from a minimization with respect to interproton separation). The units are Ry/proton.

$r_s (T = 0)$	$E^0/2$	$(E^0 + \Delta E^{(2)})/2$	$(E^0 + \Delta E^{(2)} + \Delta E^{(3)})/2$
1.5	-1.037	-1.123	-1.135
2.0	-1.076	-1.161	-1.173
2.5	-1.070	-1.154	-1.167
3.1	-1.065	-1.147	-1.160

vanish if an average over molecular axis directions is carried out as appropriate to a vibrational state.) The next contribution also vanishes, again as a consequence of inversion symmetry. Thus the contribution of a given cell to the potential decreases very rapidly at large distances from the cell (at least as fast as r^{-5}). But note also that the interactions are screened, and because of this the exact determination of $\Delta E^{(n)}$, which requires lattice summation rather than single-cell integrations, can be expected to be smaller than the equivalent error that is introduced, for instance, by calculating the Madelung energy from the familiar ion-sphere *integrations* (rather than lattice summation). For close packed structures such errors are a fraction of a percent and the errors in $\Delta E^{(2)}$, $\Delta E^{(3)}$, etc. arising from cell-cell corrections are correspondingly small.

From Fig. 4 it is quite apparent, however, that the *static lattice* results are not in good agreement with the results for the equation of state of molecular hydrogen in low pressures and densities. For example, we find an equilibrium density for the molecular solid corresponding to $r_s = 2.1$. By comparison the experimental value of r_s is 3.1 and the equilibrium density is therefore found to be about a factor of 3 too dense in the static lattice approximation. A corresponding discrepancy occurs for the cohesive energy where the calculation yields an estimate which is apparently 2 orders of magnitude too large. It must be emphasized, however, that in terms of a typical electronic energy this cohesive energy is an exceedingly small quantity.

Both of these discrepancies indicate, as we shall see, that the static lattice approximation is inadequate for the low-pressure equation of state and serve to emphasize the critical role which phonons play in this regime. In Sec. VI, we give a crude estimate of the phonon contribution to the low-density ground-state properties which shows that the phonon zero-point energy is in fact of the right magnitude to account for these discrepancies. The conclusion to be drawn is that in order to obtain good results for the molecular equation of state in the low-pressure region *both* electrons and protons must be treated self-consistently at the same time.

For small r_s the energy curve rises rapidly as we move to higher densities where the kinetic energy becomes increasingly dominant. Because of this dominance and the rapid change of the energy (compared to the phonon energies), we expect that the equation of state should be given fairly accurately by the static lattice results. (This expectation is in fact borne out explicitly when we include phonon

contributions.) Figure 5 shows the equation of state of molecular hydrogen at $T = 0$. The dashed curve shows the changes that are expected when proton dynamics are included. Also shown for comparison is the high-density point recently measured by Mao and Bell.¹⁹

B. Interpolation spacing and optic mode energy

To recapitulate briefly, for each value of r_{WS} we determine the total energy as a function of the interproton spacing, $2d$. We then minimize the energy with respect to d in order to establish the equilibrium spacing and the ground-state energy. In the low-density limit (isolated H_2 molecules) we find an interproton spacing of $1.422 a_0$ which agrees with experiment to within 1.5%. Table I gives the interproton spacing in terms of the radius of the WS sphere and in terms of the Bohr orbit. Reporting the results in these units emphasizes the fact that at low densities d is determined by the *molecular* binding energy and is independent of the WS radius. On the other hand the interproton spacing and the WS radius become comparable at high pressure which foretells the eventual shift to a monatomic basis.

Figure 6 shows the total energy as a function of

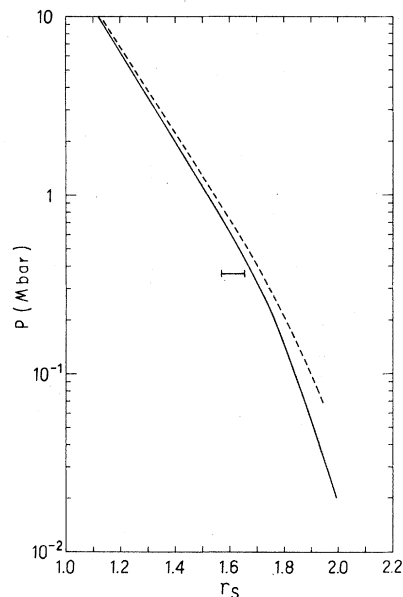


FIG. 5. Equation of state ($T = 0$) for diatomically ordered solid molecular hydrogen (full line). The dashed curve includes contributions from proton dynamics. The short bar summarizes, with uncertainties, the recent measurement of Mao and Bell (Ref. 19).

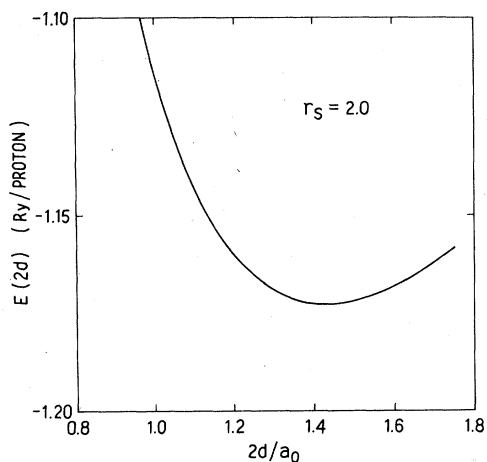


FIG. 6. Energy per proton for the molecular phase as a function of the interproton spacing, but at fixed density ($r_s = 2$).

the interproton spacing for $r_s = 2$. Within the Einstein approximation we can estimate the optic mode energy of the molecular solid from the curvature of $E(d)$ at the minimum. For the low-density limit we find $\hbar\omega_{\text{opt}} = 0.0199$ Ry/proton, which again agrees within 0.6% with the experimental result for the isolated molecule. For higher densities the optic mode energies calculated in this way are given in Table I. The energies calculated by this purely harmonic approach rise steadily with density. They do not rise as fast as an estimate of the zero-point energy would suggest. Nor do they include anharmonic corrections, which are expected to be of increasing importance at higher densities.

VI. PHONONS

For molecules of mass $2m_p$ and density $\rho/2$, we note that at sufficiently high density the basic frequencies will scale near $r_s \sim 2$ as $[4\pi(\rho/2)(2e)^2/2m_p]^{1/2}$, which is merely the plasma frequency ω_p for unpaired protons at density ρ . If m is the mass of an electron then

$$\hbar\omega_p \approx 2\sqrt{3}r_s^{-3/2}(m/m_p)^{1/2} \text{ Ry}$$

or, per proton, 0.014 Ry at $r_s = 2.0$ and 0.012 Ry at $r_s = 3$. The variation in acoustic energies alone over this range of r_s will therefore be comparable to the static binding energy. A more quantitative estimate^{20,21} can be obtained by calculating

$$\frac{1}{2} \sum_{\lambda} \sum_{\vec{k} \in \text{zone}} \hbar\omega_{\lambda}(\vec{k})$$

where, for λ designating acoustic modes we set

$\omega_{\lambda}(\vec{k}) \approx \omega_p/\epsilon^{1/2}(k)$, $\epsilon(k)$ being the wave-number-dependent dielectric function. We take the acoustic modes to be degenerate and integrate over a Debye sphere for the diatomic solid. To the result we add the longitudinal-optic-mode energy calculated as described above. Finally we add transverse-optic-mode energies estimated from zone-boundary acoustic-phonon frequencies. (These energies, though approximate, are in fact quite comparable to the results obtained by Caron.²⁰) Figure 4 shows the result of adding the approximate proton energies to the static energies: the important point is that the binding energy has dropped even further to ~ 0.007 Ry/proton.²² From this we arrive at the conclusion stated earlier that a correct determination of the low-density equation of state of condensed molecular hydrogen must necessarily require a self-consistent treatment of electron and proton degrees of freedom together.²³ In addition, any representation of the energy of high-density solid molecular hydrogen that neglects the internal structure of the molecule (and in particular the change in optic mode frequency at high pressures) must ultimately be in error.

The determination of the pressure for complete dissociation requires the addition of the phonon energies for the monatomic phase. These are also calculated from

$$\frac{1}{2} \sum_{\lambda} \sum_{\vec{k} \in \text{zone}} \hbar\omega_p/\epsilon^{1/2}(k)$$

as discussed above and the result is shown in Fig. 2. What now becomes evident is that the results of a common tangent construction (see Fig. 7) are exceedingly sensitive to the region where monatomic and diatomic curves cross. The point is made more clearly by direct reference to Fig. 7 where the ground-state energy (now as a function of r_s^3) is plotted for static monatomic (SM) and static diatomic (SD) phases. (Also indicated there is the density at which band overlap has been calculated to occur.⁴)

VII. DISCUSSION AND CONCLUSIONS

We may conclude that the density-functional approach to the electronic energies of dense hydrogen shows rather clearly the necessity for a more complete treatment of proton motion and its coupling to electrons. The results already lead to some interesting predictions for the interproton spacing and corresponding optic mode frequency as a function of density. This dynamical effect is just the most

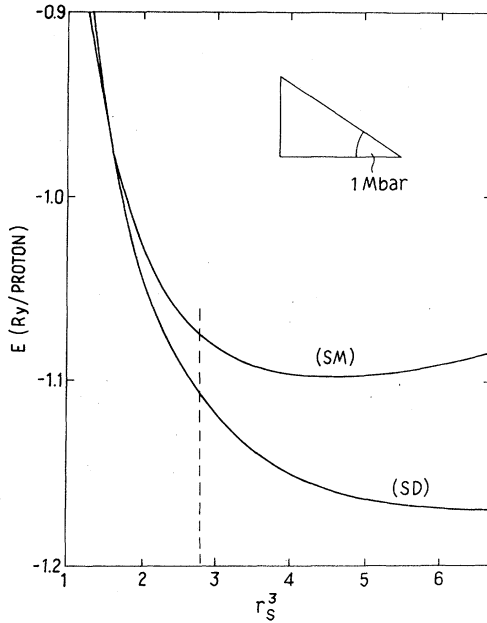


FIG. 7. Comparison of the equation of state, at $T = 0$, of static monatomic (SM) and static diatomic (SD) phases of hydrogen. Note that the abscissa is now proportional to volume: the inset shows the slope corresponding to 1 Mbar. The dashed vertical line indicates the onset of band overlap according to the results of Ref. 4.

prominent of several such effects that cannot be present in a pair-potential or multicenter description of molecular hydrogen. The results that we have obtained on the band overlap transition in hydrogen support a physical picture very similar to the description given for the behavior of diatomic molecular iodine under pressure.²⁴ The presumed second-order transitions are very similar.

It is interesting to note that the proposition of diatomic ordering in a *metallic* state of hydrogen is supported by elementary calculations based on the structural expansion method as applied to a rotationally averaged diatomic system. At each site \vec{R} of a fcc Bravais lattice we have two protons at positions $\vec{d}_{\vec{R}}$ and $-\vec{d}_{\vec{R}}$ as measured from the site. The corresponding proton density has Fourier transform

$$\rho_p(\vec{k}) = 2 \sum_{\vec{R}} e^{i\vec{k} \cdot \vec{R}} \cos \vec{k} \cdot \vec{d}_{\vec{R}}, \quad (7.1)$$

so that if $\rho(k)$ is the corresponding electron density operator, the electron-proton coupling can be written

$$H_{ep} = \frac{1}{\Omega} \sum_{\vec{k} \neq 0} \rho(-\vec{k}) \rho_p(\vec{k}) \frac{4\pi e^2}{k^2}. \quad (7.2)$$

Accordingly, to lowest order the electron response energy (or band-structure energy) calculated adiabatically is

$$\frac{1}{2\Omega} \sum_{\vec{k} \neq 0} \langle \rho(-\vec{k}) \rangle \rho_p(\vec{k}) \frac{4\pi e^2}{k^2}, \quad (7.3)$$

where $\langle \rho(-\vec{k}) \rangle$ is given by linear response theory. If the crystal has N sites, then the energy per electron, after averaging over all directions $\vec{d}_{\vec{R}}$ is²⁵

$$-\frac{1}{2N\Omega} \sum_{\vec{k} \neq 0} \frac{\epsilon(k) - 1}{\epsilon(k)} \langle \frac{1}{2} \rho_p(\vec{k}) \rho_p(-\vec{k}) \rangle \frac{4\pi e^2}{k^2}, \quad (7.4)$$

where

$$\begin{aligned} \langle \frac{1}{2} \rho_p(\vec{k}) \rho_p(-\vec{k}) \rangle = N \left[1 + \frac{\sin 2kd}{2kd} - 2 \frac{\sin^2 kd}{k^2 d^2} \right] \\ + 2N^2 \delta_{\vec{k}, \vec{K}} \frac{\sin^2 Kd}{K^2 d^2}. \end{aligned} \quad (7.5)$$

Here $\epsilon(k)$ is the dielectric function of the interacting electron gas and the $\{\vec{K}\}$ are the reciprocal-lattice vectors. Notice that the term $\langle \rho_p(\vec{k}) \rho_p(-\vec{k}) \rangle$ also appears in the Madelung energy. Thus for a given density (or r_s) the total energy per proton can be obtained by carrying out a \vec{K} sum and a straightforward numerical integral over \vec{k} . For the chosen r_s

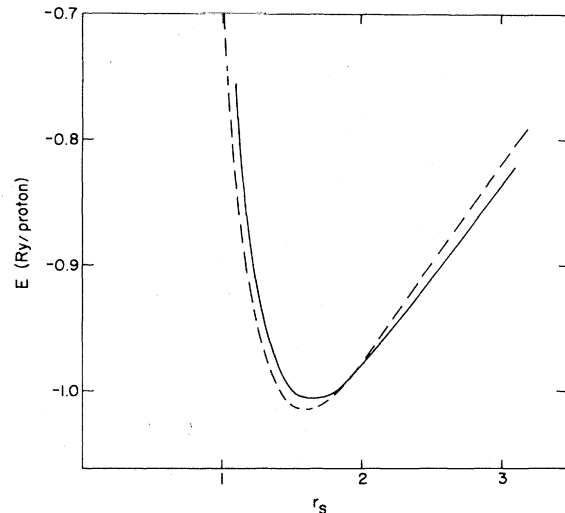


FIG. 8. Energy per proton by the structural expansion method (second order): The dashed curve is the result for a static fcc lattice. The solid curve is the result for a diatomic basis, rotationally averaged (as described in the text) and minimized with respect to variations in interproton separation.

the result is minimized with respect to d . The minimized energy corresponding to the Hubbard-Geldart-Vosko²⁶ form of $\epsilon(k)$ is shown in Fig. 8. There the energies for a monatomic fcc structure and a rotationally averaged diatomic structure are compared. The point to be made is that although the absolute energy for the diatomic phase lies above the density-functional calculation (as expected from the low-order approximation), it is nevertheless lower than the corresponding monatomic calculation in the low-density regime. The linear response method approximates the charge density near the protons quite poorly, a feature that is largely

corrected by the density-functional approach. The tendency toward pairing, though more noticeable in the density-functional calculations, is thus already apparent in the structural expansion method, and is not restricted, of course, to cubic Bravais lattices.²⁷

ACKNOWLEDGMENT

This work has been supported by the National Aeronautics and Space Administration under Grant No. NSG7487.L

-
- ¹Nor is it completely determined that the transition is necessarily solid-solid. The possibility that some phases of metallic hydrogen might be liquid, even in the ground state, has recently been proposed. See S. Chakravarty and N. W. Ashcroft, *Phys. Rev. B* **18**, 4588 (1979); K. K. Mon, G. V. Chester, and N. W. Ashcroft, *ibid.* **21**, 2641 (1980).
- ²E. Wigner and H. B. Huntington, *J. Chem. Phys.* **3**, 764 (1935).
- ³D. E. Ramaker, L. Kumar, and F. E. Harris, *Phys. Rev. Lett.* **34**, 812 (1975).
- ⁴C. Friedli and N. W. Ashcroft, *Phys. Rev. B* **16**, 662 (1977).
- ⁵M. Ross and A. K. McMahan, *Phys. Rev. B* **13**, 5154 (1976).
- ⁶W. Kohn and L. J. Sham, *Phys. Rev.* **140**, A1133 (1965).
- ⁷See, for example, N. Lang and W. Kohn, *Phys. Rev. B* **2**, 4555 (1970); **3**, 1215 (1971); B. Y. Tong, *ibid.* **6**, 1189 (1972); O. Gunnarsson, B. I. Lundqvist, and J. W. Wilkins, *ibid.* **10**, 1319 (1974); J. Harris and R. O. Jones, *J. Chem. Phys.* **68**, 1190 (1978); and H. Shore, E. Zaremba, and J. H. Rose, *Phys. Rev. B* **15**, 2858 (1977).
- ⁸We shall not be concerned with ortho-para differences here.
- ⁹B. Y. Tong, *Phys. Rev.* **122**, 1437 (1965).
- ¹⁰From structural expansion methods these energy differences are known to be quite small; see, for examples: E. G. Brovman, Yu. Kagan, and A. Holas, *Zh. Eksp. Teor. Fiz.* **61**, 2421 (1971) [*Sov. Phys.—JETP* **34**, 1300 (1972); **35**, 783 (1972)]; J. Hammerberg and N. W. Ashcroft, *Phys. Rev. B* **9**, 409 (1974); Yu. Kagan, V. V. Pushkarev, and A. Holas, *Zh. Eksp. Teor. Fiz.* **73**, 966 (1977) [*Sov. Phys.—JETP* **46**, 511 (1977)]; T. Nakamura, H. Nagara, and H. Miyagi, *Prog. Theor. Phys.* **63**, 368 (1980).
- ¹¹The details are to be found in Refs. 7 and 9.
- ¹²O. Gunnarsson and B. I. Lundqvist, *Phys. Rev. B* **13**, 4274 (1976).
- ¹³A similar starting point was used by D. A. Liberman, *Int. J. Quantum Chem. Symp.* **10**, 297 (1976).
- ¹⁴See, for example, D. Pines and P. Nozieres, *The Theory of Quantum Liquids* (Benjamin, New York, 1966), Vol. 1, Chap. 4.
- ¹⁵A. Ghazali and P. Leroux-Hugon, *Phys. Rev. Lett.* **41**, 1569 (1978); J. H. Rose, L. M. Sander, H. B. Shore, and S. Chakravarty, *Bull. Am. Phys. Soc.* **24**, 280 (1979).
- ¹⁶J. H. Rose, H. B. Shore, and L. M. Sander, *Phys. Rev. B* **21**, 3037 (1980).
- ¹⁷O. Gunnarsson, B. I. Lundqvist, and J. W. Wilkins, *Phys. Rev. B* **10**, 1319 (1974).
- ¹⁸W. Kolos and L. Wolniewicz, *J. Chem. Phys.* **49**, 404 (1968); G. Hertzberg and A. Monfils, *J. Mol. Spectrosc.* **5**, 482 (1960).
- ¹⁹H. K. Mao and P. M. Bell, *Science* **203**, 1004 (1979).
- ²⁰L. Caron, *Phys. Rev. B* **9**, 5025 (1974).
- ²¹A recent calculation of the phonon spectrum has been given by S. I. Anisimov and Yu. V. Petrov, *Zh. Eksp. Teor. Fiz.* **74**, 778 (1978) [*Sov. Phys.—JETP* **47**, 407 (1979)].
- ²²The experimental value is 0.000 585 Ry/proton.
- ²³See V. Chandrasekharan and R. D. Eppers, *J. Chem. Phys.* **68**, 4933 (1978).
- ²⁴This case has been discussed by A. K. McMahan, B. L. Hord, and M. Ross, *Phys. Rev. B* **15**, 726 (1977).
- ²⁵N. W. Ashcroft and D. C. Langreth, *Phys. Rev.* **155**, 682 (1967); see also Ref. 10.
- ²⁶J. Hubbard, *Proc. R. Soc. London Ser. A* **243**, 336 (1957); D. J. W. Geldart and S. H. Vosko, *Can. J. Phys.* **44**, 2137 (1966).
- ²⁷Highly anisotropic structures, reflecting a trend to molecule formation, have been reported in the calculations of Kagan and co-workers and also by Nakamura *et al.* (Ref. 10).